

FATIGUE CRACK PROPAGATION IN PLAIN CONCRETE BEAMS BY ACOUSTIC EMISSION TECHNIQUE

PRASHANTH M. H. *, PARVINDER SINGH † AND J. M. CHANDRA KISHEN ‡

* † Graduate Student, ‡ Professor

Indian Institute of Science, Bangalore, India

e-mail: mh_prashanth@rediff.com, psvirk.87@gmail.com, chandrak@civil.iisc.ernet.in

Key words: Fatigue, Plain concrete, Paris law, Acoustic Emission

Abstract. Fatigue crack growth in plain concrete specimens subjected to constant amplitude cyclic loading is studied. Acoustic Emission (AE) technique has been used to monitor the fatigue crack propagation. Three different sizes of geometrically similar beam specimens are prepared and are tested under three point bending (TPB) in a closed loop servo-controlled testing machine. The data such as load, displacement and CMOD from the testing of specimen for fatigue are acquired in a data acquisition systems and crack growth is continuously monitored using six AE sensors mounted on the specimen. The CMOD compliances at different cycles are measured from the load-CMOD curves and the equivalent fatigue crack lengths are determined using the compliance calibration curve obtained from FE analysis. AE parameters such as events, counts and absolute energy are used to analyze the crack growth.

1 INTRODUCTION

Civil engineering structures such as bridges, highways, offshore structures and airport runways are subjected to fatigue loading. Fatigue is a process of progressive permanent internal damage taking place in the structure. Concrete is a heterogeneous material, and consists of cement phase, aggregate phase and transition zone phase. The transition zone is the weakest zone in the concrete which contains micro-cracks even before the structure is subjected to loading. The fatigue crack propagation in concrete is much more complex due to various toughening mechanisms taking place in it. The mechanism of fatigue in concrete is not clearly understood as compared to metallic materials. Hence, it is very important to characterize the behaviour of material such as concrete subjected to fatigue loading and understand the rate of crack propagation. Hence, an attempt has been made to understand the fatigue crack

propagation in plain concrete using the acoustic emission technique. Fatigue crack propagation consists of three stages: stage 1 is the crack initiation; stage 2 is the crack propagation; and stage 3 is the unstable crack propagation leading to the final failure. Paris and Erdogan [1] have demonstrated that the crack propagation in stage 2 can be characterized through the relation

$$\frac{da}{dN} = C \Delta K^m \quad (1)$$

where da/dN is the crack growth per cycle, ΔK is stress intensity range ($K_{max} - K_{min}$). C and m are material constants which are dependent on material properties. The law has been extensively for studying fatigue crack propagation in metals and ceramics. Many researchers have attempted to apply the Paris law to describe the crack growth during the acceleration stage of fatigue crack growth in concrete. Baluch et al. [2], Perdikaris and Calomino [3]

have reported that Paris' law is a useful method for characterizing the fatigue crack growth behaviour of concrete. Bazant and Xu [4] have proposed a size adjusted Paris' law by considering the size effect on fatigue of plain concrete, as

$$\frac{da}{dN} = C \left(\frac{\Delta K}{K_{IC}} \right)^m \quad (2)$$

where, K_{IC} is the size-dependent equivalent fracture toughness which is related to the constant fracture toughness, K_{If} , as

$$K_{IC} = K_{If} \left[\frac{\beta}{1 + \beta} \right]^{1/2} \quad (3)$$

in which, β is the brittleness number [4, 5]. They have shown that Paris law coefficients are dependent on the material composition potentially explaining the large differences in their values as reported by different researchers. However, from these studies it is not clear if the Paris coefficients are material constants independent of load range. Toumi et al. [6] have carried out fatigue tests on notched concrete beam subjected to three point bending. The features of crack growth was studied by replica technique associated with scanning electron microscopy, in conjunction with the measurement of the crack mouth opening displacement. Koluru et al. [7] have studied the behaviour of concrete subjected to fatigue loading and observed that the crack growth due to constant amplitude fatigue comprises of a deceleration and an acceleration stage. They have developed analytical expressions for the crack growth in both these stages using R-curves concepts and Paris law respectively. Zhang et al. [8] have presented a semi-analytical model to study the size effect on fatigue in the bending of concrete.

The Acoustic Emission (AE) technique is a widely used tool for non destructive evaluation of materials. AE is the class of phenomena whereby transient elastic waves are generated by the rapid release of energy from a localized source or sources within a material. AE is very sensitive to the initiation and growth of cracks in materials and structures and hence has been

widely utilized for studies of materials in the laboratory. AE technique can give valuable information on what is happening inside of the material and its capability of on-line monitoring during service of structures or facilities. The acoustic emission technique offers the possibility of capturing the damage process, when and where it occurs. Shah and Chandra Kishen [9] have used the acoustic emission technique for monitoring the fatigue crack growth in plain concrete beams under three point bending configuration subjected to variable amplitude fatigue loading. There is very little information available in literature regarding the application of acoustic emission technique for studying fatigue crack growth in plain concrete. Apart from some attempts to evaluate fatigue damage for reinforced concrete slab [10] and asphalt concrete [11], very little has been reported in the literature on the use of AE technique for monitoring the fatigue crack growth in concrete.

The main objective of the present work is to study the fatigue crack propagation in plain concrete beams subjected to constant amplitude cyclic loading. Acoustic emission technique is used for monitoring the crack growth in concrete. AE data such as events, counts and absolute energy is used to analyse fracture and fatigue process. Further AE-counts data is used to check the validity of Paris model by acoustic emission.

2 EXPERIMENTAL PROGRAM

2.1 Materials and Mix Proportions

Ordinary Portland cement OPC 53 grade conforming to IS 4031-1988 is used in casting of concrete specimens. Locally available natural sand and crushed granite of 12.5 mm is used as fine aggregate and coarse aggregate respectively. The concrete mix design is done using ACI method and the mix proportion of cement, fine aggregate and coarse aggregate obtained is 1:1.86:2.61 by weight. The water to cement ratio of 0.54 is used throughout the entire mix. The slump test was done to check the workability of the mix which was in the range of 40 to

60 mm. The compressive strength of companion cubes of dimension 150mm was 51 MPa. All the specimens were cured in the water for 28 days. The geometrically similar specimens were of length to depth ratio (L/d) of 4.5, span to depth ratio (S/d) of 4, and notch to depth ratio (a_0/d) of 0.2. The notch was prepared by inserting the metal plate of 2 mm thickness at the midspan during casting. The geometric details of specimens are shown in Figure 1. The details of dimensions of small, medium and large specimens are shown in Table 1. The geometrically similar specimens are shown in Figure 2.

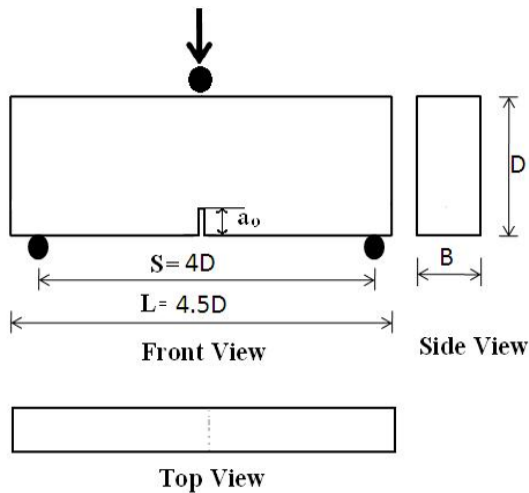


Figure 1: Details of geometry of the specimens

Table 1: Details of dimensions of beams

| Beam Size | Depth d (mm) | Span S(mm) | Length L(mm) | Notch Size a_0 (mm) |
|-----------|--------------|------------|--------------|-----------------------|
| Small | 75 | 300 | 337.5 | 15 |
| Medium | 150 | 600 | 675 | 30 |
| Large | 300 | 1200 | 1350 | 60 |



Figure 2: Geometrically similar specimens

2.2 Testing of Specimens

The specimens were tested on high stiffness loading frame of capacity 35 kN with electronically servo controlled hydraulic actuator system having digital closed loop control. The testing machine and instrumentation are shown in Figure 3. An in-built load cell of 50kN was used for measuring the load. The load point displacement is measured using linear variable displacement transformer (LVDT). The crack mouth opening displacement (CMOD) is measured using the clip gauge. Static tests are performed in CMOD control at the rate of opening of 0.001 mm/sec. Fatigue tests were of low cycle and high amplitude with load/stress ratio of $R=0.1$ as shown in Table 2 with the maximum load limit of 90% of peak load of average static monotonic test. The lower load limit was 10% of maximum load limit value. The tests were conducted in load control with sinusoidal waveform of frequency of 2 Hz. The results of load, displacement, CMOD and time are simultaneously acquired through data acquisition system.

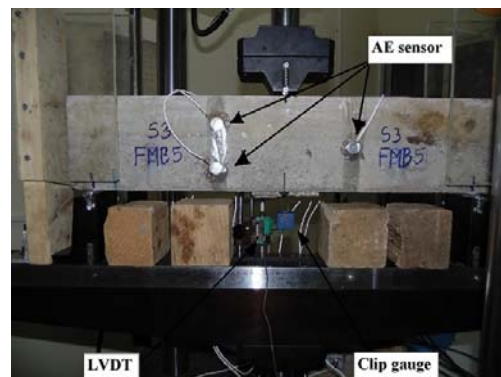


Figure 3: Testing of beam specimen with accessories such as clip gauge, LVDT and AE sensors

Table 2: The details of maximum and minimum load limits in fatigue testing

| Beam | Peak(kN) | Pmax(kN) | Pmin(kN) |
|--------|----------|----------|----------|
| Small | 2.80 | 2.50 | 0.25 |
| Medium | 4.00 | 3.60 | 0.36 |
| Large | 6.67 | 6.00 | 0.60 |

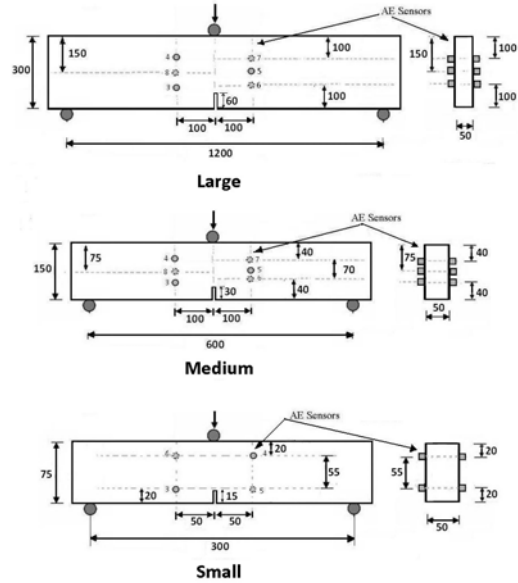


Figure 4: AE sensor location for large, medium and small size specimens

The details of instrumentation used for acquisition of AE data is shown in Figure 4. In order to obtain a 3D location of AE-events, six AE-sensors are mounted on the specimen for medium and large specimen in a triangulation scheme with three sensors in the front face and three sensors in back face. Four sensors are mounted on the small specimen with two sensors in front face and two sensors in back face. The AE data such as hits, events, energy, absolute energy, signal strength, spatial positions, amplitude and time are simultaneously acquired using data acquisition system during the experiments. The resonant type differential sensors R6D, having a diameter and height of 19 mm and 22 mm, respectively are used in the experimental work. The high vacuum silicon grease has been used as couplant. The AE signals are amplified with a gain of 40 dB in a (PAC) pre-amplifier. An eight-channel AE-WIN for SAMOS E2.0 (Sensor based Acoustic Multichannel Operating System), developed by Physical Acoustics Corporation (PAC)-USA has been used for AE data acquisition. A threshold of 40 dB, which is normally used for concrete is adopted.

3 RESULTS AND DISCUSSION

3.1 Results from Mechanical Testing

The experimental data acquired on load, CMOD and mid-span vertical displacement during the tests is analysed. The plot of load vs CMOD obtained from the testing is as shown in Figure 5. From these plots the slope of unloading portion is computed for each cycle which is termed as CMOD compliance and its inverse referred as flexural stiffness. Figure 6 shows the plot of variation of stiffness with number of cycles. From the Figure it is observed that three distinctive zones are present. In the first zone, during the initial cycles there is a higher drop in stiffness followed by second zone where there is a gradual drop and in the third stage a sudden drop of the stiffness of beam specimen occurs. Similar kind of trends were obtained for the large medium and small size specimen as shown in Figure 6. The effective crack lengths were determined from the finite element code ATENA for the beam specimen with three point loading for different notch to depth (a/d) ratios and the respective compliances are computed and compliance calibration curves are obtained. From the measured compliances at different load cycles, the corresponding effective crack lengths are estimated using the compliance cal-

ibration curve for that specimen. The plot of relative crack length versus the number of cycles for different size of specimens is shown in Figure 7. From these crack lengths, the fatigue crack growth rate (da/dN) is computed for the relative crack length a/D as shown in the Figure 8. From the plots, it can be observed that the crack growth rate has a deceleration stage followed by acceleration stage until failure. This observation was made by Kolluru et al. [7] where there is a distinctive bendover point ($a_{bendover}$) which was found to exist which separates the rate of crack growth from deceleration to acceleration. This bendover occurs at the same crack length as the inflection point in the observed in Figure 7. From Figure 8 the deceleration stage typically ends at 20 to 35 % of the specimens fatigue life.

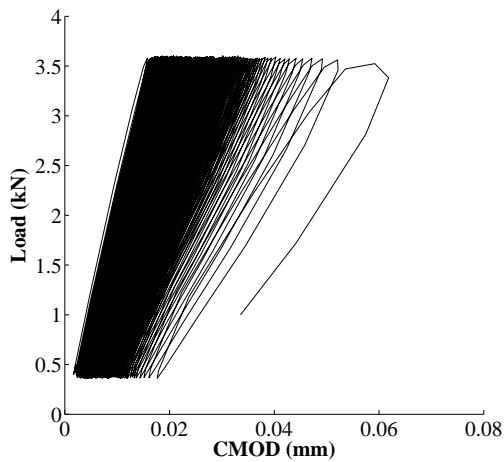


Figure 5: Load vs CMOD plot of medium specimen

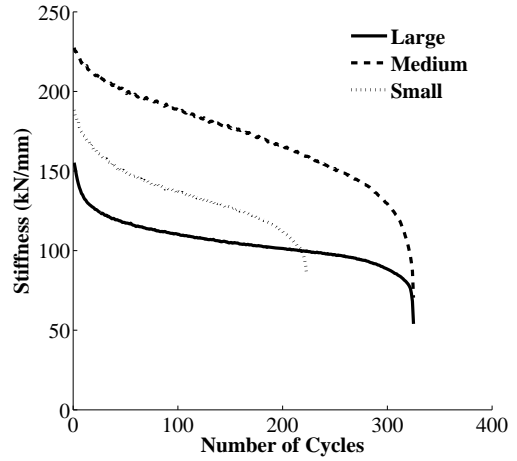


Figure 6: Stiffness vs Number of cycles

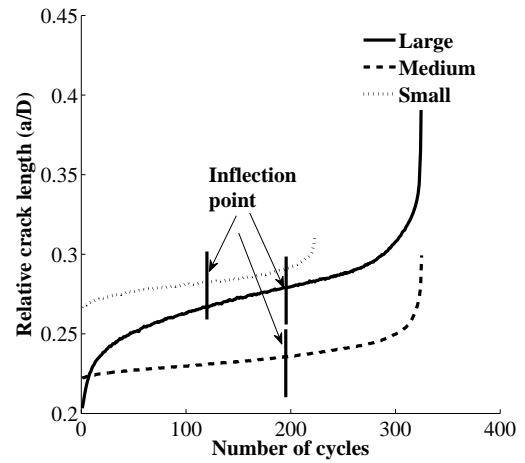


Figure 7: Relative crack length vs Number of cycles

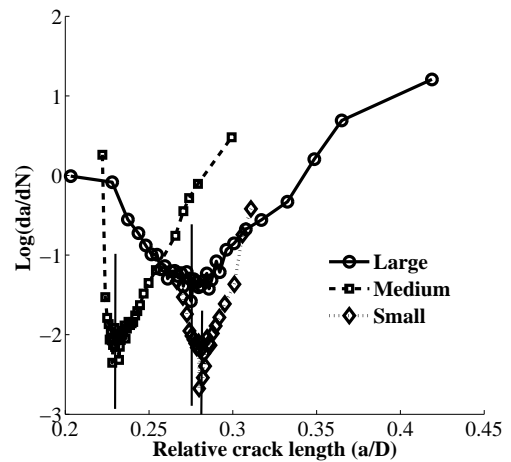


Figure 8: Crack growth rate during fatigue loading

3.2 Results on Acoustic Emission (AE)

3.2.1 AE Events AE counts and Absolute AE energy

AE events are a result of micro cracking in the concrete material and spread of these events indicate the micro cracking distribution with various other toughening mechanisms taking place with the subsequent formation of fracture process zone. Figure 9 shows the 3D location of AE events for small, medium and large specimens under fatigue loading. The number of AE events occurring for different specimens are indicated in these figures. It is seen that the cluster of AE events has progressed up to mid depth of the specimen. The occurrence of number of AE events increases with the increase in the size, because of increase in the ligament length. The events at failure in fatigue is very less when compared to number of events in static monotonic testing as shown in Table 3. The AE counts are number of signal pulses crossing the threshold. Counts depend on the magnitude of the source event, but they also depend strongly on the acoustic properties of the material. From Figures 10 and 11, it can be observed that plots can be divided into three zones. In the first zone there is sudden rise of events and counts due to loading in first few cycles in which all the events and counts are released, as such the specimen is suddenly loaded and comparable to static monotonic testing. In the second zone the events and counts are released in steady rate. In the third zone when the crack reaches the critical crack size, there is very rapid increase in the events and counts indicating the failure of specimen. A similar trend is observed for small medium and large size specimens. Hence sudden rise of events and counts gives very important prediction for fatigue failure in case of practical application (e.g. online bridge monitoring).

Absolute energy is defined as the integral of the squared voltage signal divided by the reference resistance (10k-Ohm) over the duration of AE wave form. This is the true energy measure of AE hit. The unit of absolute energy is

Atto joules. The absolute energy (aJ) recorded by each AE sensor depends on the spatial location of event. Nearer the event to the AE sensor, higher is the amount of absolute energy released to that sensor. The cumulative absolute AE energy at failure in fatigue is very less when compared to cumulative absolute AE energy of static monotonic testing as shown in Table 4. From Figure 12 it is observed that the rate of increase of absolute energy is lower in the first zone of loading. This could be due to the formation of micro cracks which generate low absolute energy. In the second zone, the absolute energy released from each micro crack formation in every cycle builds up which is observed in an increase in the slope or few limited sharp risers indicating that the acceleration stage has started. This is due to the rate of increase in events in the formation of fracture process zone. The third zone indicates higher energy release rate due to the formation of macro cracks. The flatter portions of the plot corresponds to macro crack propagation during which less absolute energy is released which is continued to be observed till the specimen fails. From Figure 12, it can be observed that general trend of absolute energy with number of cycles is similar for all specimen sizes.

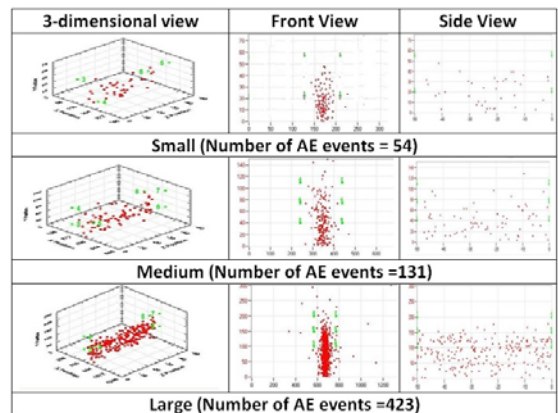


Figure 9: Location for AE events for small, medium and large size specimens during failure in fatigue loading

Table 3: The results of AE events from monotonic static and fatigue tests

| Beam Size | Events Static | Events Fatigue |
|-----------|---------------|----------------|
| Small | 1600 | 54 |
| Medium | 2900 | 131 |
| Large | 6050 | 423 |

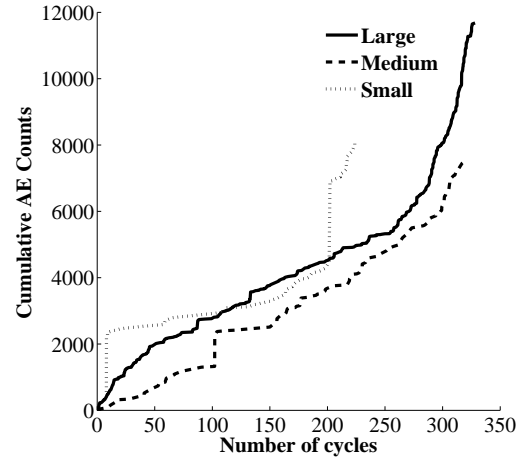


Figure 11: AE counts vs Number of cycles

Table 4: The results of Absolute AE energy from monotonic static tests and fatigue tests

| Beam Size | Absolute Energy(aJ) Static | Absolute Energy(aJ) Fatigue |
|-----------|----------------------------|-----------------------------|
| Small | 7.3E+08 | 2.7E+06 |
| Medium | 7.6E+08 | 3.1E+06 |
| Large | 12.9E+08 | 2.5E+06 |

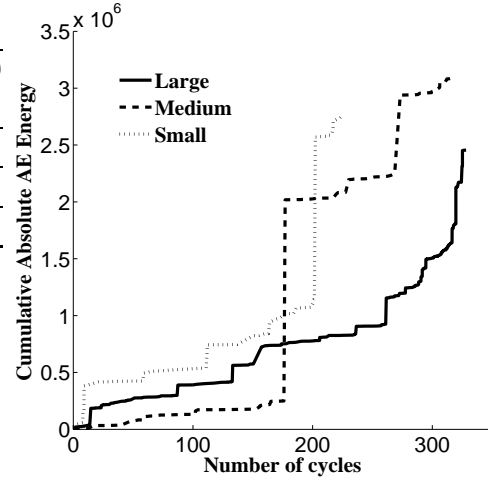


Figure 12: Absolute AE energy vs Number of cycles

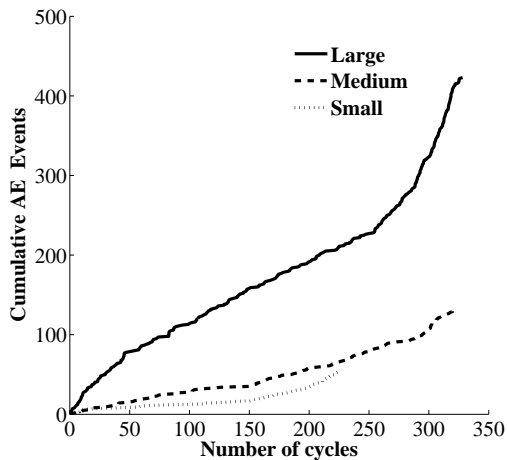


Figure 10: AE events vs Number of cycles

3.2.2 AE Counts as a validation to Paris model

The AE crack signal is an indication that some part of the released energy due to the crack propagation is transformed into an elastic wave. From this, we can suppose that the energy of the emitted elastic wave is directly proportional to the energy release rate, which is a fracture mechanics parameter that occurs as a result of crack propagation [12]. Dunegan et al. [13] have suggested that the total cumulative AE count, N_{AE} is directly proportional to the volume of the plastic area at the crack tip as

shown in Equation 4.

$$N_{AE} = CV_p \quad (4)$$

where, N_{AE} is the total cumulative AE count, and V_p is the volume of the plastic area at the crack tip. In addition, Morton et al. [14] have reported an experimental relationship between the total cumulative AE count and the stress intensity factor range ΔK for aluminum as

$$\frac{dN_{AE}}{dN} = A(\Delta K)^l \quad (5)$$

where, dN_{AE}/dN is the rate of increase of AE counts per cycle and where A and l are constants that are determined by experiment. In this experiment, an attempt is made to apply the AE count rate (dN_{AE}/dN) with the SIF range (ΔK) for plain concrete as shown in Figure 13. It is observed that the AE count rate follows the Paris law (Equation 5) quite well. The constants A and l are obtained and shown in the Table 5.

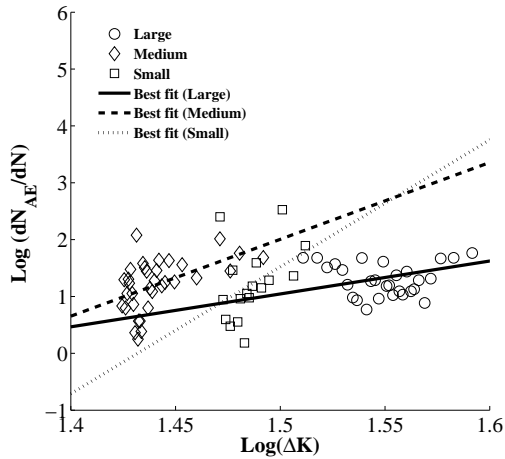


Figure 13: AE count rate vs SIF range

Table 5: Constants A and l of Paris equation

| Beam | l | A |
|--------|-------|-------|
| Small | 22.33 | 31.98 |
| Medium | 13.51 | 18.27 |
| Large | 7.69 | 5.78 |

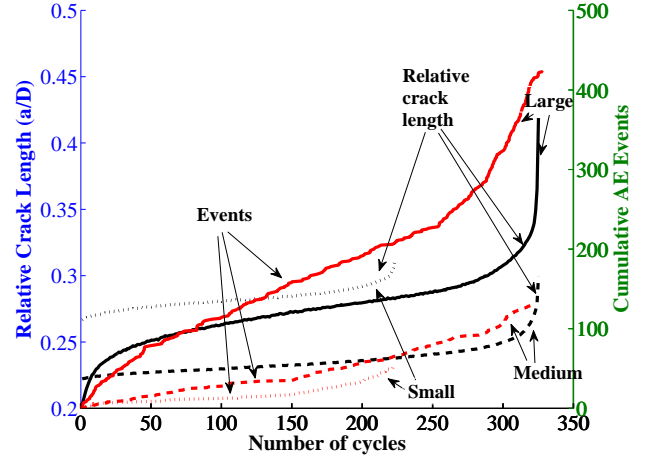


Figure 14: Cumulative AE events and relative crack length vs Number of cycles

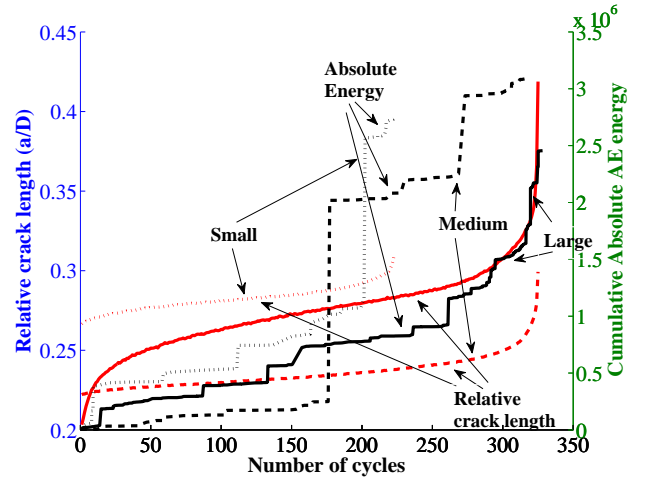


Figure 15: Cumulative Absolute AE energy and relative crack length vs Number of cycles

Figure 14 shows the relative crack length and AE events with increasing load cycles for all the sizes of specimens. It is seen that there is an increase in the number of AE events with corresponding increase of relative crack length indicating the damage and cracking taking place. It can be observed that the sudden rise in events and relative crack depth when the beam specimen is near to failure. Similar trend is observed for all sizes of specimen.

Figure 15 shows the relative crack length and absolute AE energy with increasing load cycles for different sizes of specimens. It is seen that there is an increase in the absolute AE energy

with corresponding increase of relative crack length. It can be observed that there is rise in absolute energy or change in the slope at the point of inflection of relative crack depth vs number of cycles which is the indication of acceleration stage. When the beam specimen is near to failure the flatter portions indicate the macro crack propagation during which less absolute energy is released and steep risers indicating sudden rise of addition of microcracks. Similar trend is observed for all sizes of specimen.

4 CONCLUSIONS

In this study, the Acoustic Emission (AE) technique has been used for monitoring the fatigue crack growth in plain concrete specimens subjected to constant amplitude cyclic loading. Beam specimens of different sizes are prepared and tested as three-point bending (TPB) in a closed loop servo-controlled testing machine under fatigue loading. The fatigue crack growth is continuously monitored using six AE-sensors mounted on the specimen.

From the results it is observed that there is a decrease in the flexural stiffness from the beginning to the failure of the specimens and three distinctive zones were observed. It is observed that the crack growth rate has a deceleration stage followed by acceleration stage until failure. There is a distinctive bendover point ($a_{bendover}$) which was found to exist which separates the rate of crack growth from deceleration to acceleration. This bendover occurs at the same crack length as the inflection point. The deceleration stage typically ends at 20 to 35 % of the specimens fatigue life.

From the results, it is observed that three zones could be identified. In the first zone there is sudden rise of events and counts due to loading during the first few cycles in which all the events and counts are released. In the second zone, the events and counts are released at steady rate. In the third zone when the crack reaches the critical crack size, there is very rapid increase in the events and counts indicating the failure of specimen. It is seen that there is a increase in the absolute AE energy with

corresponding increase of relative crack length. When the beam specimen is near to failure the flatter portions indicate the macro crack propagation during which less absolute energy is released and steep risers indicating sudden rise of addition of microcracks.

AE-events, AE-counts and Absolute AE energy can represent the amount of cracking and damage that is undergoing during the fatigue loading. It is observed that acoustic emission is very important tool to predict the fatigue crack length as well as failure as the events and counts will increase very rapidly toward the fatigue failure. To measure or observe the fatigue crack propagation in concrete is very difficult, because the crack will not be seen unless it has become critical and when it becomes critical, in fraction of seconds the specimen will break.

REFERENCES

- [1] P. Paris and F. Erdogan. A critical analysis of crack propagation laws. *Transactions of ASME Journal of Basic Engineering*, 85:528–534, 1963.
- [2] M. H. Baluch, A. B. Qureshy, and A. K. Azad. Fatigue crack propagation in plain concrete. In *Proceedings of SEM/RILEM International Conference on Fracture of Concrete and Rock, Houston*, pages 80–87, June 1987.
- [3] Philip C. Perdikaris and Anthony M. Calomino. Kinetics of crack growth in plain concrete. In *Proceedings of SEM/RILEM International Conference on Fracture of Concrete and Rock, Houston*, pages 64–69, June 1987.
- [4] Zdenek P. Bazant and Kangming Xu. Size effect in fatigue fracture of concrete. *ACI Materials Journal*, 88(4):390–399, July-August 1991.
- [5] Zdenek P. Bazant and William F. Schell. Fatigue fracture of high-strength concrete and size effect. *ACI Materials Journal*, 90(5):472–478, September-October 1993.

- [6] A Toumi, A Bascoul, and A Turatsinze. Crack propagation in concrete subjected to flexural cyclic loading. *Materials and Structures*, 31(7):451–458, 1998.
- [7] Subramaniam V. Kolluru, Edward F. O’Neil, John S. Popovics, and Surendra P. Shah. Crack propagation in flexural fatigue of concrete. *Journal of Engineering Mechanics*, 126(9):891–898, September 2000.
- [8] Jun Zhang, Victor C Li, and Henrik Stang. Size effect on fatigue in bending of concrete. *Journal of materials in civil engineering*, 13(6):446–453, 2001.
- [9] Santosh G Shah and JM Chandra Kishen. Use of acoustic emissions in flexural fatigue crack growth studies on concrete. *Engineering Fracture Mechanics*, 87:36–47, 2012.
- [10] S. Yuyama, Z.-W. Li, M. Yoshizawa, T. Tomokiyo, and T. Uomoto. Evaluation of fatigue damage in reinforced concrete slab by acoustic emission. *NDT & International*, 34:381–387, 2001.
- [11] Youngguk Seo and Y. Richard Kim. Using acoustic emission to monitor fatigue damage and healing in asphalt concrete. *KSCE Journal of Civil Engineering*, 12(4):237–243, 2008.
- [12] Ki Bok Kim, Dong Jin Yoon, Jung Chae Jeong, and Seung Seok Lee. Determining the stress intensity factor of a material with an artificial neural network from acoustic emission measurements. *NDT & E International*, 37:423–429, 2004.
- [13] H. L. Dunegan, D. O. Harris, and C. A. Tatro. Fracture analysis by use of acoustic emission. *Engineering Fracture Mechanics*, 1(1):105–122, 1968.
- [14] T. M. Morton, S. Smith, and R. M. Harrington. Effect of loading variables on the acoustic emission of fatigue crack growth. *Experimental Mechanics*, 14(5):208–213, May 1974.